Elastic scattering analysis of α and ^{3}He particles on ^{12}C and ^{16}O using a complex folded potential

S. A. E. Khallaf, A. M. A. Amry, and S. R. Mokhtar
Department of Physics, Faculty of Science, Assiut University, Assiut, Egypt
(Received 2 January 1997)

The angular distribution of differential cross sections for α and ^{3}He projectiles elastically scattered from ^{12}C and ^{16}O are calculated at the energy range from 25 to 217 MeV. The double folding model with an energy-target density dependent Jeukenne, Lejeune, and Mahaux effective nucleon-nucleon interaction is used to obtain both real and imaginary parts of the central optical potential. The dependence of the potential on densities of projectile and target nuclei in a factorized form is considered. Good fits to the experimental data are obtained. Nuclear rainbow scattering is also observed and discussed. [S0556-2813(97)05310-7]

PACS number(s): 24.10.Ht, 25.55.Ci

I. INTRODUCTION

Recently, Hogenbirk *et al.* [1,2] used, for the first time, the double folding (DF) procedure, taking into account the density dependent factorization, with the Jeukenne, Lejeune, and Mahaux (JLM) effective nucleon-nucleon *NN* interaction [3], which is energy and target density dependent, to analyze elastic and inelastic scattering of α particles on ^{36}S at 31.61 MeV up to $\Theta_{\text{c.m.}}=70°$. Using JLM interaction has the advantage that it enables one to obtain the real part as well as the imaginary part of the α nucleus interaction by the DF model. They obtained the density dependent parameters for the real and imaginary parts of optical model potential (OMP). They also pointed out that as their work was confident to only one experiment at a relatively low beam energy, it would be of interest to extend such an analysis to experiments at higher beam energies and on different nuclei in order to study the general validity of JLM interaction in DF calculations. On the other hand, Pecina *et al.* [4] chose DF model together with JLM effective interaction to construct elastic optical potentials and form factors for inelastic scattering of ^{7}Be, ^{8}B+^{12}C at 40 MeV per nucleon.

In the present work, we consider elastic scattering of ^{3}He (from 25 to 217 MeV) and α particles (from 32.2 to 172.5 MeV) on ^{12}C and ^{16}O targets. At lower energies, ^{3}He and α scattering show anomalous large angle scattering (ALAS) [5,6], where angular distribution becomes more sensitive to detailed shape of the real part of the optical potential at smaller radii. Such details cannot be reproduced with standard Woods-Saxon (WS) potential and discrete ambiguities of the potential were observed [7]. At higher energies, ^{3}He and α particles seem to be reasonably transparent and refractive rainbow scattering is observed [8–10]. Precise determination of optical potential which fits ALAS at low energies and rainbow scattering at high energies [11] allows more investigation of internuclear interactions at short distances [12].

The DF model has been widely used to analyze elastic scattering processes, where an effective (*NN*) interaction based upon a realistic *G* matrix (or *t* matrix) is folded into nuclear matter distributions of projectile and target nuclei. The M3Y effective *NN* interaction has been widely used in DF model by folding only the real part of OMP, while the imaginary part is usually taken in WS form. Applications of M3Y interaction in elastic scattering of α and helion particles were done [13]. Fitting was obtained by normalizing the real part with renormalization factors close to unity. M3Y interaction failed beyond a certain energy $E_\alpha \geqslant 100$ MeV for α-elastic scattering, where it could not reproduce the rainbow angles [14]. The potential had to be multiplied by a renormalization factor $N_R=0.55$ to fit the data. M3Y interaction has only a weak incident energy dependence, arising from one boson exchange. It has no explicit dependence on the nuclear density. The nuclear density dependence, arising from Pauli principle effects on the overlapping region, is dominant at high energies.

Kobos *et al.* [14,15] modified M3Y interaction by factorizing it to radial dependent (original M3Y interaction) and density dependent (depending on density distributions of projectile and target) terms and the resultant model is called DDM3Y interaction. Application of DDM3Y interaction on elastic scattering of α particles and heavy ions [10,14–17] shows that this interaction could neither describe elastic scattering of α particles from nuclei with target mass number $A_T>40$, in the energy range of 20 to 43 MeV per nucleon (where the renormalization for the real part $N_R=1.3$), nor scattering of heavy ions, in the energy range of 4 to 9 MeV per nucleon (where $N_R=0.6$ to 0.8). This may be due to the weakness of energy dependence in DDM3Y interaction.

Chaudhuri [18] tried to solve this problem by factorizing the density dependent term into target and projectile dependent terms. This factorization was characterized by two parameters, the strength and the density dependent parameters. These parameters were found to be equal for both α particles and heavy ion projectiles.

The DF procedure is rarely used in the ^{3}He particle-nucleus reactions, since the increase of break up effect [19] of ^{3}He and the presence of rainbow angles [14] lead to smaller values of N_R. Cook and Griffiths [19] used M3Y interaction to describe the trition and helion particles scattering from different nuclei. They proposed that the smaller values of N_R may be related to the break up effect for these projectiles.

The goal of this work is, firstly, to check the validity of

JLM interaction specially using an imaginary DF potential for elastic scattering of light projectiles (^{3}He and α particles) at a wide energy range, secondly, to find the consistent density dependent parameters for ^{3}He and α-particles elastic scattering.

II. FORMALISM

The central optical potential consists of a real part and an imaginary part. In the framework of DF form which is considered here, the real $V_{\rm opt}$ and imaginary $W_{\rm opt}$ potentials for nucleus-nucleus elastic scattering are [4]

$$V_{\rm opt}(r,E)=N_R\int\int d^3\mathbf{r}_1 d^3\mathbf{r}_2\rho_1(\mathbf{r}_1)\rho_2(\mathbf{r}_2)v_{\rm eff}(\mathbf{S},\rho_1,\rho_2,E) \tag{2.1}$$

and

$$W_{\rm opt}(r,E)=N_I\int\int d^3\mathbf{r}_1 d^3\mathbf{r}_2\rho_1(\mathbf{r}_1)\rho_2(\mathbf{r}_2)w_{\rm eff}(\mathbf{S},\rho_1,\rho_2,E), \tag{2.2}$$

where $\rho_1(\mathbf{r}_1)$ and $\rho_2(\mathbf{r}_2)$ are the nucleon density distribution of the target and projectile nuclei, respectively, $v_{\rm eff}$ and $w_{\rm eff}$ are the total density- and energy-dependent effective NN interaction for the real and imaginary parts, respectively, $\mathbf{S}=\mathbf{r}+\mathbf{r}_2-\mathbf{r}_1$, E is the projectile energy per nucleon in lab frame and $\mathbf{r}$ is the separation vector between the centers of mass for the projectile and target nuclei. N_R and N_1 are renormalization factors of the DF potentials. The total nucleon-nucleon effective interaction for the real $v_{\rm eff}$ and imaginary $w_{\rm eff}$ parts can be factorized as follows [1,20]:

$$v_{\rm eff}(\mathbf{S},\rho_1,\rho_2,E)=h(\mathbf{S})\nu_1(\rho_1,E)f_1(\rho_2,E)$$

for the real part,

$$w_{\rm eff}(\mathbf{S},\rho_1,\rho_2,E)=h(\mathbf{S})\nu_2(\rho_1,E)f_2(\rho_2,E) \tag{2.3}$$

for the imaginary part,

where $\nu_i(\rho_1,E)$ $[i=1,2]$ represents the JLM effective NN interaction which is based on the realistic g-matrix from Reid soft core using improved local density approximation (LDA). This effective interaction parametrizes the energy and density dependence (of the target only), for the nucleon-nucleus scattering. This parametrization consists of isoscalar, isovector, and Coulomb correction of the complex OMP. The JLM interaction was adjusted to the energy range $10<E<160$ MeV. In the present work, we consider the isoscalar component only (symmetric $N=Z$ and uncharged nuclear matter). We multiply the imaginary part of JLM by the effective mass correction to represent the true nonlocality of the OMP. This procedure led to improvement in the mean free path of the propagation of nucleon inside the nucleus [21]. These interactions are given in details elsewhere [3]. The projectile density dependence for the real and imaginary parts is chosen as follows [22]:

$$f_i(\rho_2,E)=\begin{cases}1-\beta_R(E)\rho_2^{2/3}, & i=1 \text{ for the real part}\\ 1-\beta_I(E)\rho_2^{2/3}, & i=2 \text{ for the imaginary part.}\end{cases} \tag{2.4}$$

The parameters β_R and β_I represent the factorized projectile density dependence for real and imaginary potentials, respectively. The radial dependence $h(\mathbf{S})$ is taken in the Gaussian form as [1–3]

$$h(\mathbf{S})=\frac{1}{(t\sqrt{\pi})^3}\exp(-S^2/t^2), \tag{2.5}$$

with $t=1.2$ fm. In the present work the nuclear matter distribution functions of targets $\rho_1(\mathbf{r}_1)$ and projectiles $\rho_2(\mathbf{r}_2)$ are chosen in the following integrable forms:

$$\rho_1(r_1)=\rho_{\circ 1}(1+A_1r_1^2)\exp(-B_1r_1^2),$$

with $A_1=0.49877$ fm^{-2}, $B_1=0.37408$ fm^{-2} for ^{12}C nucleus [23] and $A_1=0.64566$ fm^{-2}, $B_1=0.32283$ fm^{-2} for ^{16}O nucleus [23], and

$$\rho_2(r_2)=\rho_{\circ 2}\exp(-B_2r_2^2)$$

with $B_2=0.7014$ fm^{-2} for α-particles [1], $B_2=0.5505$ fm^{-2} for ^{3}He-particles [24]. The constants $\rho_{\circ i}$ $(i=1,2)$ are calculated from the normalization condition

$$\int \rho_i(r_i)d^3\mathbf{r}_i=A_i,$$

where A_i represents the mass number of the considered nucleus.

III. ANALYSIS

Introducing the central real and imaginary potentials given by Eqs. (2.1) and (2.2) into the DWUCK4 computer program [25], the angular distribution of differential cross sections for ^{3}He and α-particles elastic scattering from ^{12}C and ^{16}O nuclei are calculated. The real and imaginary folded potentials are calculated at 0.1 fm intervals up to maximum radii of 15 fm. Table I lists the sets of elastic scattering data being analyzed. Here we must point out that the measurements of $\alpha+^{16}$O elastic data at 104 MeV is multiplied by an experimental normalization constant equals 0.729 suggested by Michel *et al.* [7] and confirmed by Abele and Staudt [11]. The experimental data of ^{3}He$+^{12}$C elastic scattering differential cross sections at 41 MeV [39,40] are not extrapolated smoothly from the 40.9 MeV [37] data. It differs appreciably in the scattering angle ranges $40°<\Theta_{\rm c.m.}<55°$ and $\Theta_{\rm c.m.}>90°$. Similar inconsistencies are found in case of ^{3}He$+^{16}$O between 41 MeV [30,39] and 40.9 MeV [37] in the scattering angle range $102°<\Theta_{\rm c.m.}<115°$.

Folding model which fits data uses the potential

$$U(r,E)=V_{\rm opt}(r,E)+iW_{\rm opt}(r,E)+\left(\frac{\hbar}{m_\pi c}\right)^2 \times(V_{\rm so}+iW_{\rm so})\frac{1}{r}\frac{df_{\rm so}(r)}{dr}\overline{L\cdot\sigma}+V_C(r),$$

where V_C is Coulomb potential of a homogeneously charged sphere with radius $R_C=r_cA_T^{1/3}$, where $r_c=1.26$ fm for α scattering on ^{12}C and ^{16}O, while $r_c=1.4$ fm for ^{3}He scattering on ^{12}C except at $E_{\rm lab}^{^3{\rm He}}=82.1$ MeV, $r_c=1.25$ fm and r_c

TABLE I. Experimental data used in the present analysis of α and ^{3}He-particles elastic scattering on ^{12}C and ^{16}O nuclei.

Reaction	$\alpha+^{12}$C							$\alpha+^{16}$O						
E_{lab} (MeV)	54.1	90	104	139	145	166	172.5	32.2	40.4	54.1	65	80.7	104	146
Ref.	[5]	[10]	[26]	[27]	[9]	[28]	[9]	[11]	[11]	[5]	[29]	[11]	[26]	[11]
Reaction	^{3}He$+^{12}$C							^{3}He$+^{16}$O						
E_{lab} (MeV)	27.4	41	72	82.1	98	119	217	25	33.3	40.9	60			
Ref.	[30]	[30]	[31]	[32]	[10]	[33]	[34]	[35]	[36]	[37]	[38]			

$=1.3$ fm for ^{3}He scattering on ^{16}O except at $E_{lab}^{^3He}=25$ MeV, $r_c=1.4$ fm. The standard WS shape function for spin orbit term $f_{so}(r)$ is used in case of elastic scattering of ^{3}He particles due to its half integer spin. For ^{12}C and ^{16}O nuclei, the spin orbit term has a small contribution to data. In general, spin orbit potential affects differential cross sections only at $\Theta_{c.m.}>100°$ [33,35]. Therefore, spin orbit term is not included in our analysis, except at $E_{lab}^{(^3He,^{12}C)}=72$ MeV where it is used for WS and DF analysis since the data was extended to very large angles.

We calculated the elastic scattering differential cross section, using (1) adequate phenomenological WS potentials taken from literature, (2) the derived real part only of JLM interaction, i.e., JLM(R), while the imaginary part is taken in WS form, and (3) both the derived real and imaginary parts of JLM interaction, i.e., JLM(R+I).

In this paper, we discuss the effect of density dependent projectile term given by Eq. (2.4), where fitting is performed by two sets. First, we investigated the absence of projectile density term on cross section data, i.e., we put $\beta_R=\beta_I=0$ (no density dependent projectile term NDDP), and found out that $N_R\neq N_I\neq 1$ which means that potential had to be projectile density dependent. Second, we consider the effect of density dependent projectile term (DDP) where β_R and β_I are changed to obtain the best fit to data. The calculated differential cross sections for the best fitting, representing the second set are shown in figures.

IV. RESULTS AND DISCUSSIONS

A. α scattering

α scattering data at energies from 54.1 to 172.5 MeV are fitted using the above procedure. The fits are shown in Figs. 1–4 and the associated parameters for the two sets (NDDP and DDP) at various energies for JLM(R) and JLM(R+I) are given in Tables II and III, respectively. Good fits are obtained using JLM(R+I) potential at all energies. For low energies ($E_{lab}^{(\alpha,^{16}O)}=32.2$ Mev), see Fig. 3, good fits for ALAS are found. Also, good fitting is found for higher energies where the rainbow scattering is observed as shown in Figs. 1, 2, and 4. The only poor fit is found at $E_{lab}^{(\alpha,^{12}C)}=54.1$ MeV, Fig. 2. This is consistent with the results of Abele *et al.* [5] who used the DF real potential in their analysis using DDM3Y interaction. They claimed ''the differential cross sections for strongly deformed nuclei like ^{11}B and ^{12}C are beyond the scope of an optical model analysis to interpret the angular distributions at this energy.''

The JLM(R) potential gives good fitting to data at forward angles but at large angles its prediction decreases more rapidly than the experimental data. Table II lists the parameters of JLM(R) for the two sets. (1) NDDP set ($\beta_R=0$) where we find N_R constant at all energies for the same reaction ($N_R=0.79$ for $\alpha+^{12}$C, and $N_R=0.74\pm0.02$ for $\alpha+^{16}$O). (2) DDP set where we find $N_R=1$ for all reactions and $\beta_R=0.75$ for $\alpha+^{12}$C and $\beta_R=0.93\pm0.02$ for $\alpha+^{16}$O at all energies. Chaudhuri [18] analyzed α-particle-nucleus reaction using FDDM3Y interaction, where he found that β_R is constant in the energy range from 104 to 172.5 MeV for α scattering on different targets. In the present JLM(R) DF

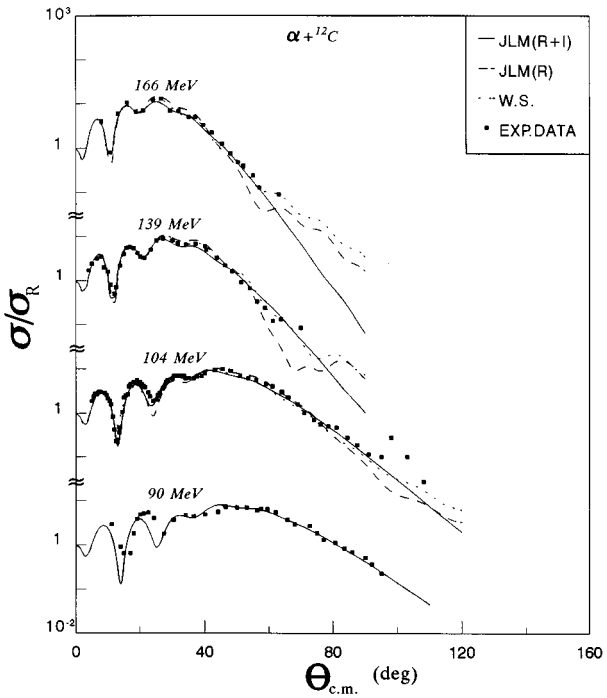

FIG. 1. The differential cross sections as ratio to Rutherford, for the elastic scattering of α particles on ^{12}C reaction at $E_{lab}^{\alpha}=90$, 104, 139, and 166 MeV reproduced by JLM(R+I), JLM(R), and WS potentials, compared with the experimental data taken from references shown in Table I. For DF potentials the density dependent sets of parameters given in Table II for JLM(R) and Table III for JLM(R+I) are considered. Solid curves are JLM(R+I), dashed curves are JLM(R), and dotted curves are WS calculations.

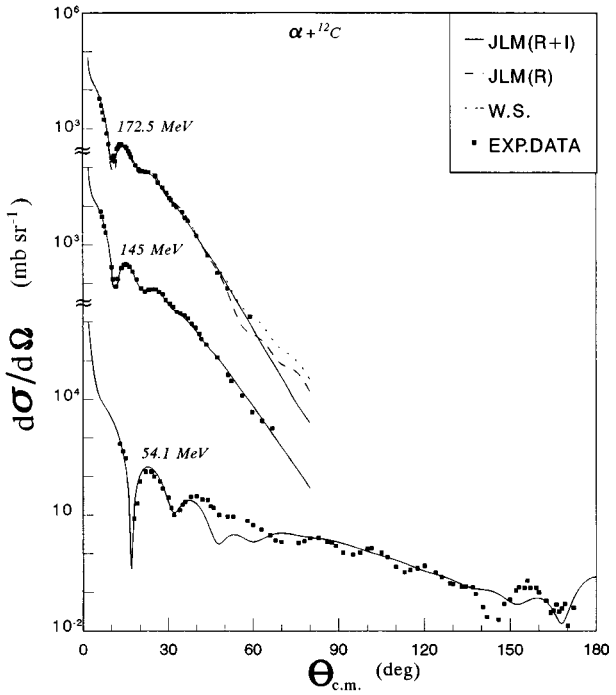

FIG. 2. The same as Fig. 1 but for differential cross sections at $E^{\alpha}_{\rm lab}=54.1$, 145, and 172.5 MeV.

work, there is a difference between the values of β_R for $\alpha+{}^{12}$C and $\alpha+{}^{16}$O reactions. This may indicate the necessity of readjustment of the imaginary WS potential to keep β_R constant for different targets and to modify the differential elastic scattering prediction at backward angles.

Table III lists the parameters of best fitting for JLM(R+I). The first set gives NDDP case ($\beta_R=\beta_I=0$),

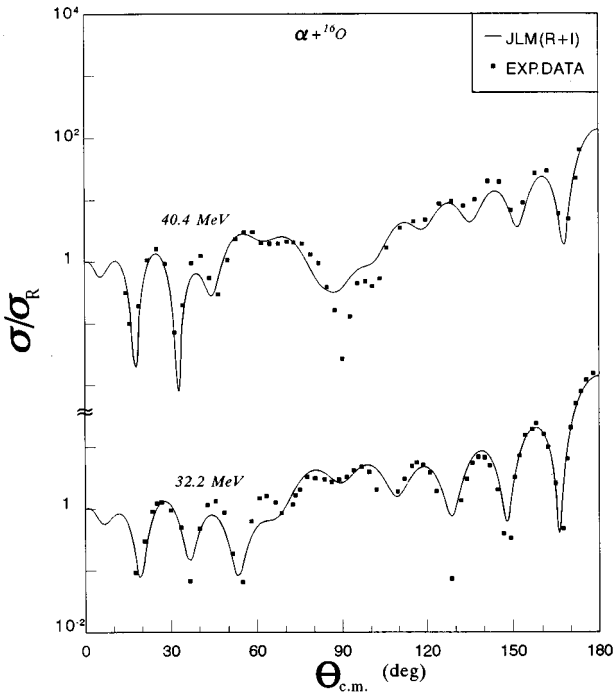

FIG. 3. The same as Fig. 1, but for the elastic scattering of α particles on ^{16}O reaction at $E^{\alpha}_{\rm lab}=32.2$, and 40.4 MeV reproduced by JLM(R+I) only for the density dependent set given in Table III.

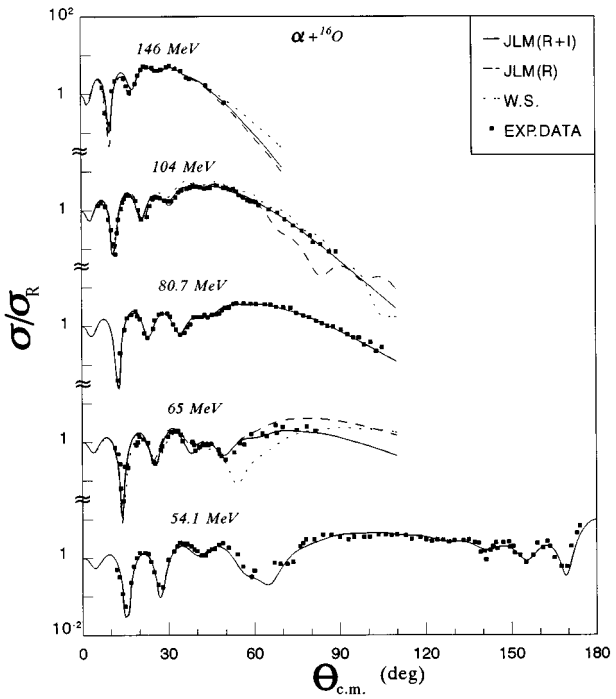

FIG. 4. The same as Fig. 1, but for the elastic scattering of α particles from ^{16}O reaction at $E^{\alpha}_{\rm lab}=54.1$, 65, 80.7, 104, and 146 MeV.

where we find that N_R is 0.72 ± 0.02 for the two reactions at all considered energies, indicating that the real part of JLM(R+I) potential describes well the energy dependence of α scattering in the energy range 32.2–172.5 MeV. The values of N_I change from 0.6 at 90 MeV to 0.8 at 172.5 MeV for $\alpha+{}^{12}$C, while they change from 0.33 at 32.2 MeV to 0.72 at 146 MeV for $\alpha+{}^{16}$O, which is far from unity at lower energies. These low values of N_I agree with those obtained by others [40] who used JLM interaction for nucleon-nucleus reactions where they concluded that JLM(I) is too absorptive for light nuclei at energies less than 50 MeV per nucleon. This means that the highest energy considered here for α reaction is in this absorptive range for JLM(I).

The second set in Table III represents the DDP case ($N_R=N_I=1$), where β_R is found to be constant at unity. This means that the projectile density dependent term for the real part is energy independent in the investigated energy range. The values of β_I, however, decrease with increasing energy. This dependence of β_I on the projectile energy may be related to the imaginary part of JLM potential which is too absorptive for light nuclei at lower energies where at these energies the probability of other nonelastic channels are enhanced.

Abele and Staudt [11] analyzed $\alpha+{}^{16}$O and $\alpha+{}^{15}$N elastic scattering up to 150 MeV by folding the real and imaginary parts of OMP using DDM3Y interaction taking into account the dispersion relation which is connected to the imaginary part of the OMP. They found good agreement between the experimental and calculated differential cross sections. Our results seem to be better than theirs, since in their work N_R was greater than unity (1.236–1.42) and N_I had higher values so that it reaches at some energies 3.667.

TABLE II. Best fit parameters of the real folded JLM(R) and WS imaginary potentials for α-particle scattering. The parameters of WS imaginary part are taken from references shown in the last column. Set (1) for NDDP parameters and set (2) for DDP parameters.

	$E_{\rm lab}$ (MeV)	N_R	β_R	W_v	r_v	a_v	Ref.
$\alpha+^{12}$C	104	(1) 0.79	0.0	13.8	1.91	0.5	[27]
		(2) 1.0	0.75				
	139	(1) 0.79	0.0	16.9	1.85	0.47	[27]
		(2) 1.0	0.75				
	166	(1) 0.79	0.0	14.7	1.86	0.48	[27]
		(2) 1.0	0.75				
	172.5	(1) 0.79	0.0	16.8	1.076	0.53	[9]
		(2) 1.0	0.75				
$\alpha+^{16}$O	65	(1) 0.75	0.0	14.9	1.64	0.77	[42]
		(2) 1.0	0.95				
	104	(1) 0.76	0.0	13.68	1.92	0.40	[42]
		(2) 1.0	0.90				
	146	(1) 0.72	0.0	14.7	1.8	0.77	[42]
		(2) 1.0	0.95				

Another analysis was performed by Li Qing-Run and Yong-Xu [41] for elastic scattering of $\alpha+^{16}$O in the energy region from 25 to 55 MeV, using single folding (SF) model with α-α interaction, $v_{\alpha\text{-}\alpha}$, considering the four α-particle model of ^{16}O. This folding potential provided a satisfactory description of the experimental data even though N_R was 0.87 and 0.82 for 32.2 and 54.1 MeV, respectively.

From our results, we find that the analysis with JLM(R+I) agrees well with the results of Chaudhuri [18] where β_R is constant in the energy range $65 \leqslant E^{\alpha}_{\rm lab} \leqslant 172.5$ MeV. This result suggests that β_R is constant too for different target nuclei, i.e., the values of β_R may depend only on the projectile density in this energy range. At lower energies β_R decreases with decreasing energy for $\alpha+^{16}$O reaction.

B. ^{3}He scattering

The calculated differential cross sections for ^{3}He scattering data at energies from 27.4 to 217 MeV are shown in Figs. 5–8. We can see that JLM(R+I) potential gives a satisfactory fit at $E^{^3{\rm He}}_{\rm lab} \geqslant 60$ MeV. At lower energies, JLM(R+I) fails to reproduce the differential cross section in limited regions and this failure shifts toward smaller scattering angles and becomes shorter as energy increases, while JLM(R) potential gives a better fitting at these energies (Figs. 5 and 8). This behavior may be related to the validity of JLM(I) interaction at lower energies, since the valid energy range is $10 \leqslant E \leqslant 160$ where E represents the incident energy per nucleon of the projectile. At higher energies, when the rainbow scattering occurs, the JLM(R+I) gives better descriptions of data than JLM(R). Generally, the fit-

TABLE III. Best fit parameters of the real and imaginary folded potentials, JLM(R+I), for α-particle scattering. Set (1) for NDDP parameters and set (2) for DDP parameters.

	$E_{\rm lab}$ (MeV)	N_R	β_R	N_I	β_I		$E_{\rm lab}$ (MeV)	N_R	β_R	N_I	β_I
$\alpha+^{12}$C	54.1	(1) 0.73	0.0	0.6	0.0	$\alpha+^{16}$O	32.2	(1) 0.74	0.0	0.33	0.0
		(2) 1.0	1.0	1.0	1.8			(2) 1.0	0.85	1.0	2.9
	90	(1) 0.72	0.0	0.61	0.0		40.4	(1) 0.74	0.0	0.38	0.0
		(2) 1.0	1.05	1.0	1.58			(2) 1.0	0.92	1.0	2.7
	104	(1) 0.715	0.0	0.64	0.0		54.1	(1) 0.72	0.0	0.44	0.0
		(2) 1.0	1.0	1.0	1.47			(2) 1.0	0.9	1.0	2.23
	139	(1) 0.7	0.0	0.74	0.0		65.0	(1) 0.74	0.0	0.63	0.0
		(2) 1.0	1.0	1.0	0.87			(2) 1.0	1.0	1.0	1.6
	145	(1) 0.72	0.0	0.7	0.0		80.7	(1) 0.73	0.0	0.58	0.0
		(2) 1.0	1.0	1.0	1.1			(2) 1.0	1.0	1.0	1.7
	166	(1) 0.72	0.0	0.77	0.0		104	(1) 0.72	0.0	0.64	0.0
		(2) 1.0	1.0	1.0	0.98			(2) 1.0	1.0	1.0	1.44
	172.5	(1) 0.73	0.0	0.8	0.0		146	(1) 0.72	0.0	0.72	0.0
		(2) 1.0	1.0	1.0	0.95			(2) 1.0	1.0	1.0	1.0

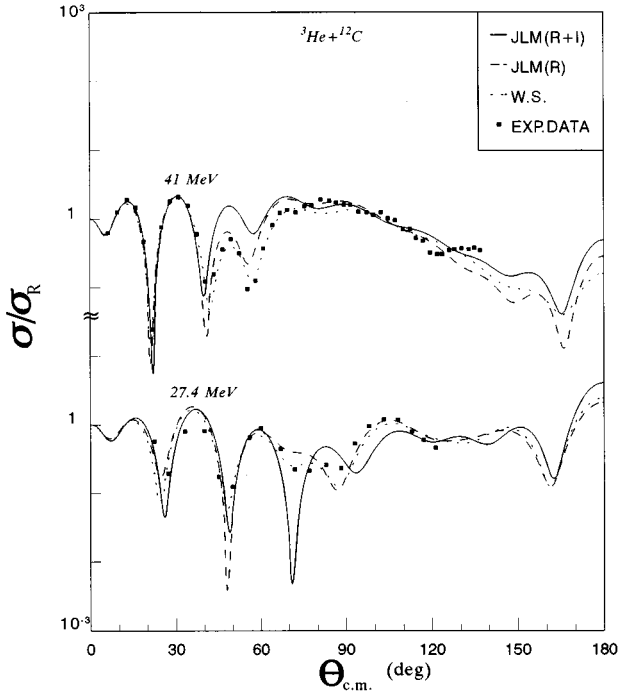

FIG. 5. The same as Fig. 1, but for ^{3}He+^{12}C reaction at 27.4 and 41 MeV. The density dependent parameters are given in Table IV for JLM(R) and Table V for JLM(R+I).

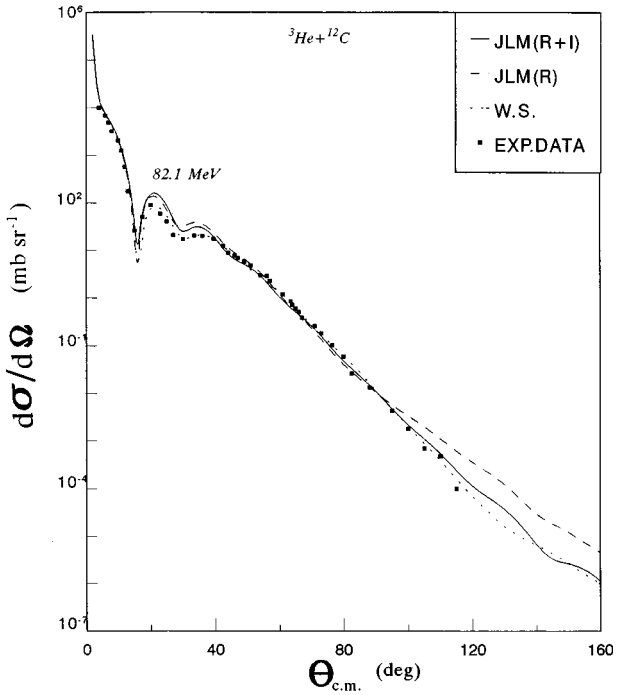

FIG. 7. The same as Fig. 5, but for the differential cross section at 82.1 MeV.

ting for ^{3}He-nucleus scattering is less satisfactory than for α-nucleus scattering. This may be related to increase of the breakup effect [19] elastic transfer [43] and nonelastic channels for this reaction.

Table IV displays the parameters of fitting for JLM(R) potential.

(1) In NDDP set ($\beta_R=0$) for all energies below 217 MeV, the values of N_R are around 0.83 ± 0.07 for both ^{3}He+^{12}C and ^{3}He+^{16}O scattering reactions.

(2) In DDP set ($N_R=1$), the values of β_R are around 0.75 ± 0.05 for ^{3}He+^{12}C scattering, except for $E_{\rm lab}^{(^3{\rm He},^{12}{\rm C})}=72$ MeV ($\beta_R=0.6$) which may be related to increase of elastic transfer reaction at large angles [43]. For ^{3}He+^{16}O reaction, β_R takes different values around unity.

At $E_{\rm lab}^{(^3{\rm He},^{12}{\rm C})}=217$ MeV, we can see that the two sets combine in one set with parameters: $N_R=1$ and $\beta_R=0$. We

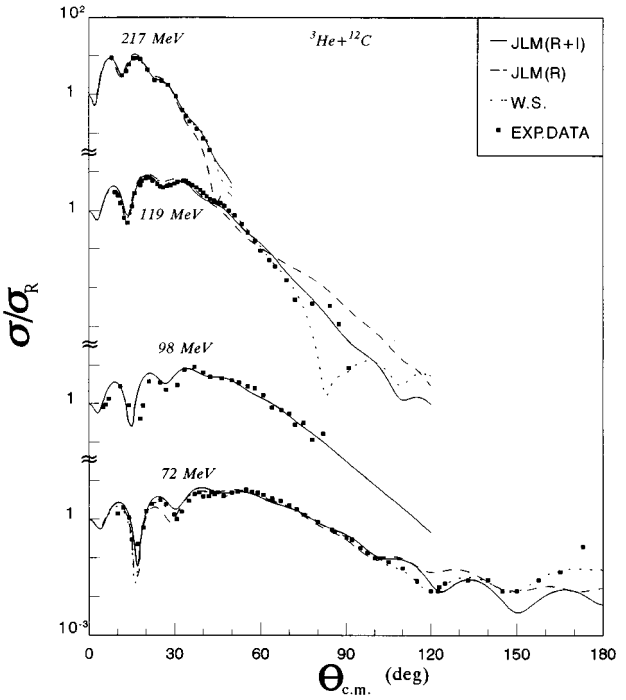

FIG. 6. The same as Fig. 5, but at 72, 98, 119, and 217 MeV.

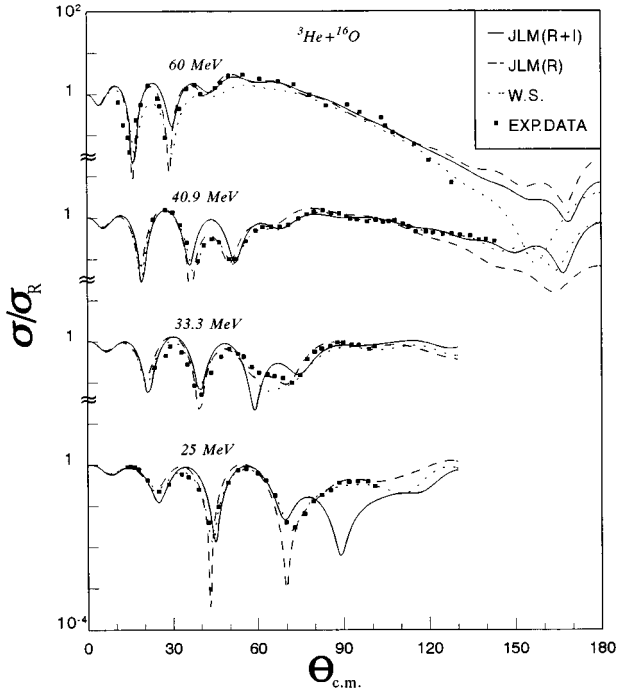

FIG. 8. The same as Fig. 5, but for ^{3}He+^{16}O reaction at 25, 33.3, 40.9, and 60 MeV.

TABLE IV. Best fit parameters of the real folded JLM(R) and WS imaginary potentials for ^{3}He-particle scattering. The parameters of WS imaginary part are taken from references shown in the last column. At $E_{\rm lab}^{(^3{\rm He},^{12}{\rm C})}=72$ MeV the readjusted spin orbit parameters are $V_{\rm so}=0.31$ MeV, $r_{\rm so}=1.62$ fm, and $a_{\rm so}=1.91$ fm. At $E_{\rm lab}^{(^3{\rm He},^{16}{\rm O})}=40.9$ MeV the imaginary parameters are slightly readjusted from those given in Ref. [39] to get the fitting. Set (1) for NDDP parameters and set (2) for DDP parameters.

	$E_{\rm lab}$ (MeV)		N_R	β_R	W_v	r_v	a_v	W_s	r_s	a_s	Ref.
^{3}He+^{12}C	27.4	(1)	0.875	0.0				12.27	1.693	0.622	[30]
		(2)	1.0	0.75							
	41	(1)	0.9	0.0				14.74	1.339	0.724	[30]
		(2)	1.0	0.7							
	72	(1)	0.9	0.0	4.58	2.17	0.98	9.9	1.268	0.55	[31]
		(2)	1.0	0.6							
	82.1	(1)	0.85	0.0				14.3	1.17	0.81	[32]
		(2)	1.0	0.8							
	119	(1)	0.85	0.0				15.64	1.133	0.787	[33]
		(2)	1.0	0.8							
	217	(1)	1.0	0.0	20.7	1.58	0.67				[34]
		(2)	1.0	0.0							
^{3}He+^{16}O	25	(1)	0.775	0.0	5.9	2.302	0.593				[35]
		(2)	1.0	1.27							
	33.3	(1)	0.8	0.0				10.81	1.572	0.701	[19]
		(2)	1.0	1.12							
	40.9	(1)	0.83	0.0				11.0	1.535	0.73	[39]
		(2)	1.0	0.97							
	60	(1)	0.79	0.0	4.460	2.289	0.558	7.411	1.064	0.756	[38]
		(2)	1.0	1.15							

must refer to the experimental data at that energy is given up to $\Theta_{\rm c.m.}=45°$ as shown in Fig. 6. The value of β_R may be changed if the data is extended to greater angles, where JLM(R) calculated differential cross section decreases rapidly for $\Theta_{\rm c.m.}>35°$. At $E_{\rm lab}^{(^3{\rm He},^{12}{\rm C})}=72$ MeV the imaginary parameters, which give good fitting in case of WS potential [31], do not give good fitting in case of JLM(R) potential. Therefore, at 72 MeV, we use another set of imaginary part [31] and the spin orbit parameters are readjusted to reproduce data at large angles, this new set (imaginary and spin orbit parameters given in Table IV and its caption) leads to a better fitting with data as shown in Fig. 6.

For ^{3}He+^{16}O, different sets of imaginary parameters given in Ref. [35] for 25 MeV, Ref. [19] for 33.3, and Ref. [38] for 60 MeV are used. At 40.9 MeV, we use the WS parameters given by Trost *et al.* [39]. They analyzed data at 41 MeV, and got a better fit than Alvarez and Pálla [37] at 40.9 MeV. In the present work, the imaginary parameters given in Table IV are slightly changed from those used in WS analysis [39] to fit the data at 40.9 MeV.

The parameters for the best fitting of JLM(R+I) potential are shown in Table V. At $E_{\rm lab}^{(^3{\rm He},^{12}{\rm C})}=72$ MeV, again we adjust the spin orbit parameters (shown in the caption of Table V) to be slightly different than the above JLM(R) treatment. In NDDP set ($\beta_R=\beta_I=0$) (we are concerned with energies above 41 MeV), N_R is approximately constant around $0.81+0.04$ even at 217 MeV, except at $E_{\rm lab}^{(^3{\rm He},^{12}{\rm C})}=98$ MeV where there is a sudden increase in N_R to 0.94, while the values of N_I increase with energy. In DDP set ($N_R=N_I=1$), the same constancy around unity (comparing with α reaction) of β_R is found except at $E_{\rm lab}^{(^3{\rm He},^{12}{\rm C})}=98$ MeV (decreases to 0.4), while the parameter β_I has a decreasing behavior with increasing energy tending to zero at 119 and 217 MeV as in case of α reactions considered here.

V. REACTION CROSS SECTION

Another quantity, which measures the validity of JLM effective interaction, is the total reaction cross section σ_R (absorption cross section), since it is strongly correlated to the imaginary potential and it gives us an additional guide to the discussion. For the composite projectiles and heavy ions as stated in Ref. [44], there are strong absorption at low incident energies with higher values of σ_R which simply falls off as the energy increases and stays around a certain value for each intermediate or high energy reaction as *transparency effect*. The DWUCK4 program [25] gives the values of σ_R for each case of our analysis, i.e., for WS, JLM (R), and JLM(R+I) potentials as $\sigma_R^{\rm WS}$, $\sigma_R^{\rm JLM(R)}$ and $\sigma_R^{\rm JLM(R+I)}$, respectively. We are interested in the values of $\sigma_R^{\rm JLM(R+I)}$ because it includes the derived imaginary part and no WS imaginary potentials are needed, so JLM(R+I) potential gives us the ability to discuss the dependence of σ_R on incident energies without the ambiguities (discrete and continuous) which appear in analysis using WS potentials. Quantitatively, we compare σ_R deduced from elastic scattering data using optical model in previous three forms used here together.

Table VI contains the values of σ_R of DDP set. The simi-

TABLE V. Best fit parameters of the real and imaginary folded potentials, JLM(R+I), for ^{3}He-particle scattering. At $E_{lab}^{(^3He,^{12}C)}=72$ MeV the readjusted spin orbit parameters are $V_{so}=0.32$ MeV, $r_{so}=1.59$ fm, and $a_{so}=0.183$ fm. Set (1) for NDDP parameters and set (2) for DDP parameters.

	E_{lab} (MeV)		N_R	β_R	N_I	β_I		E_{lab} (MeV)		N_R	β_R	N_I	β_I
^{3}He+^{12}C	27.4	(1)	0.85	0.0	0.84	0.0	^{3}He+^{16}O	25	(1)	0.77	0.0	0.73	0.0
		(2)	1.0	1.0	1.0	1.2			(2)	1.0	1.27	1.0	2.5
	41	(1)	0.85	0.0	0.88	0.0		33.3	(1)	0.77	0.0	0.7	0.0
		(2)	1.0	1.0	1.0	0.9			(2)	1.0	1.12	1.0	2.1
	72	(1)	0.85	0.0	0.85	0.0		40.9	(1)	0.81	0.0	0.72	0.00
		(2)	1.0	0.9	1.0	1.2			(2)	1.0	1.0	1.0	1.6
	82.1	(1)	0.81	0.0	0.87	0.0		60	(1)	0.82	0.0	0.8	0.0
		(2)	1.0	1.0	1.0	0.7			(2)	1.0	1.05	1.0	1.4
	98	(1)	0.94	0.0	0.98	0.0							
		(2)	1.0	0.4	1.0	0.2							
	119	(1)	0.81	0.0	1.0	0.0							
		(2)	1.0	1.0	1.0	0.0							
	217	(1)	0.81	0.0	1.05	0.0							
		(2)	1.0	1.0	1.05	0.0							

larity between the values of σ_R^{WS} and $\sigma_R^{JLM(R)}$ is noticed for several reactions. This is expected since the imaginary part, which is strongly correlated to σ_R, is the same for WS and JLM (R) analysis. This is not the case for ^{3}He+^{12}C reaction at 72 MeV or for ^{3}He+^{16}O reactions where we use different sets of parameters for the imaginary part. As a result of these differences, the reaction cross sections calculated using WS and JLM(R) potentials may not give a good description of transparency effect in the investigated energy range.

The results of JLM(R+I) potential give a good description for σ_R decrease as energy increases. But, it can be noticed for $\alpha+^{16}$O reaction, at lower energies the values of $\sigma_R^{JLM(R+I)}$ slightly increase up to 65 MeV, since at these energies there is a strong absorption of the incident particles increasing with energy. This absorption tends to saturation at a limited energy range and then decreases as energy increases. This behavior of $\sigma_R^{JLM(R+I)}$ may be compared with the associated volume integral per nucleon $J_I/4A_T$ for the

TABLE VI. The reaction cross sections σ_R, in mb, deduced by various potentials for considered reactions.

E_{lab} (MeV) $\alpha+^{12}$C	54.1	90	104	139	145	166	172.5
σ_R^{WS}			837.91	768.68		722.34	754.58
$\sigma_R^{JLM(R)}$			831.19	767.89		723.16	751.24
$\sigma_R^{JLM(R+I)}$	946.75	853.43	826.86	787.88	760.16	726.15	715.77
E_{lab} (MeV) $\alpha+^{16}$O	32.2	40.4	54.1	65	80.7	104	146
σ_R^{WS}				1059.9		943.31	1042.1
$\sigma_R^{JLM(R)}$				1087.1		915.41	1039.4
$\sigma_R^{JLM(R+I)}$	1045.3	1056.7	1055.2	1060.4	1009.7	966.54	898.76
E_{lab} (MeV) ^{3}He+^{12}C	27.4	41	72	82.1	98	119	217
σ_R^{WS}	1128.5	1023.7	961.47	885.68		795.33	646.38
$\sigma_R^{JLM(R)}$	1112.1	1034.1	1063.6	901.33		800.8	646.66
$\sigma_R^{JLM(R+I)}$	1019.2	974.65	851.99	834.77	810.66	750.53	561.67
E_{lab} (MeV) ^{3}He+^{16}O	25	33.3	40.9	60			
σ_R^{WS}	1236.8	1222.9	1161.8	1212.3			
$\sigma_R^{JLM(R)}$	1242.1	1207.2	1206.6	1125.5			
$\sigma_R^{JLM(R+I)}$	1109.6	1098.6	1087.8	1022.7			

TABLE VII. Comparison between JLM(R+I) parameters (renormalization factors and density dependent parameters) around 8 MeV per nucleon for the three considered systems.

		N_R	β_R	N_I	β_I
$\alpha+^{16}$O	(1)	1.00	0.85	1.00	0.00
E_{lab}=32.2 MeV	(2)	1.00	0.85	0.70	0.00
	(3)	1.14	0.40	0.90	0.00
^{3}He+^{12}C	(1)	1.00	1.00	1.00	0.00
E_{lab}=27.4 MeV	(2)	1.00	1.00	0.70	0.00
^{3}He+^{16}O	(1)	1.00	1.27	1.00	0.00
E_{lab}=25 MeV	(2)	1.00	1.27	0.70	0.00

imaginary part of the optical potential for $\alpha+^{16}$O elastic scattering, given by Michel *et al.* [7] and Abele and Staudt [11] where it increases linearly with energy up to about 55 MeV and tends to saturation beyond that energy.

VI. COMPARISON WITH THE PREVIOUS ANALYSIS OF JLM INTERACTION

As we stated before, Hogenbirk *et al.* [1,2] used JLM(R+I) interaction to analyze $\alpha+^{36}$S reaction at 31.61 MeV, i.e., 7.9 MeV/N. They used the same factorization of the densities used here for JLM interaction, but they found that the density dependence of the imaginary part for that reaction equals zero, and the other parameters were given as $N_R=1.145$, $N_I=0.956$, and $\beta_R=0.4$. The analyzed data were fitted at forward angles only where $\Theta_{c.m.}<70°$ since there was no available data greater than 70°. These parameters are different from these of the present work, specially for density dependent parameters β_R and β_I at similar energy per nucleon. In this section, we discuss the validity of JLM interaction at backward angles and the effect of density parameters at these angles around an energy equals 8 MeV/N, i.e., for the following reactions $\alpha+^{16}$O at 32.2 MeV, ^{3}He+^{12}C at 27.4 MeV, and ^{3}He+^{16}O at 25 MeV.

The present work shows that JLM(R+I) fails to reproduce the differential cross section at backward angles for ^{3}He+nucleus scattering at $\Theta_{c.m.}>70°$ (Figs. 5 and 8). In the case of $\alpha+^{16}$O reaction, JLM(R+I) reproduces the data but with a higher value of β_I (in DDP set) or with a very small value of N_I (for NDDP set). In case of $\alpha+^{16}$O reaction we test the potential by using parameters very close to those of Hogenbirk, listed as set (3) in Table VII, and two other sets given by the following.

(1) We put $\beta_I=0$ with the same parameters of the best fitting given in Table III.

(2) We change N_I to smaller values than unity keeping $\beta_I=0$.

The latter two sets are performed for ^{3}He+nucleus scattering. The results are given in Fig. 9 and the parameters in Table VII. For $\alpha+^{16}$O reaction, the three sets give a satisfactory fitting at forward angles up to 60°, the differences are observed for greater angles. For ^{3}He+^{12}C and ^{3}He+^{16}O reactions, the fitting with data are shown in Fig. 9 with different sets of Table VII up to $\Theta_{c.m.}\simeq 70°$ and the significant differences are found at greater angles. We can see that the imaginary part as a whole and the imaginary density dependent parameters β_I for α and ^{3}He particles scattered from light nuclei affects only at angles greater than 70°, and to get the true density dependence of parameters for the imaginary part, data should be extended for the backward scattering angles. This may reflect the importance of the parameter β_I. So, the JLM(R+I) interaction must be used carefully at low energies, around 10 MeV per nucleon, since it does not give a good description for the data for all systems as a results of its intrinsic behavior at these energies.

VII. CONCLUSION

Through this paper, the angular distributions of the elastic scattering differential cross sections of different projectiles (^{3}He and α) on (^{12}C and ^{16}O) targets at different energies are analyzed. The JLM effective NN interaction (with real and imaginary folding potentials) is used with density dependent

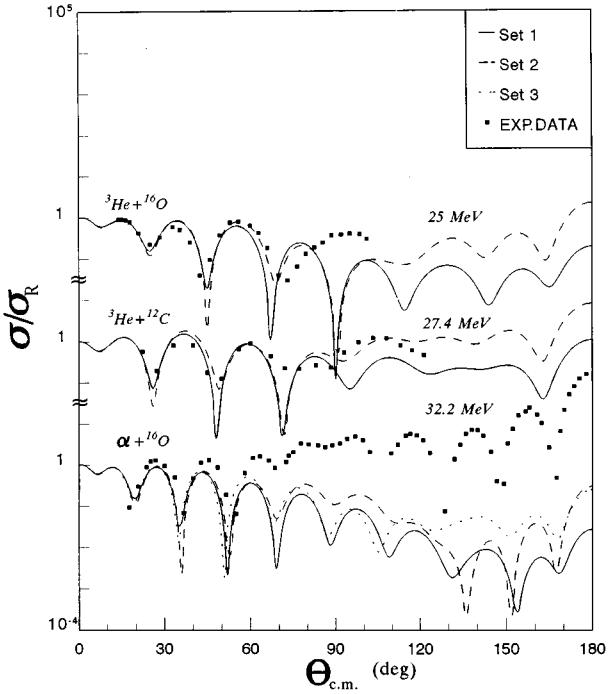

FIG. 9. Comparison between the differential cross sections for three systems at comparable energy per nucleon for JLM(R+I). Solid and dashed curves represent set (1) and set (2) of parameters given in Table VII for all systems. The dotted curve represents set (3) of Table VII for $\alpha+^{16}$O reaction at 32.2 MeV.

effect considered as a factorized density dependence. The following conclusions may be drawn.

(1) For all investigated reactions at different energies, the resulting calculated differential cross sections reproduced by JLM(R+I) potential (including the projectile density dependent term in DF potential) agree well with the experimental data for energies above 13 MeV per nucleon, at lower energies it gives a good fit with data for $\alpha+{}^{16}$O reaction and fails at limited angles for ^{3}He reactions.

(2) The predictions of differential cross sections of JLM(R) potential for these projectiles are less satisfactory at energies above 25 MeV/N.

(3) In case of JLM(R+I) potential:

(a) The renormalizations N_R and N_I for the real and imaginary potentials, respectively, at energies $E_{\rm lab}\geqslant 16$ MeV/N, are equal to unity indicating that JLM(R+I) potential describes well the energy dependence of the real and imaginary parts in this energy range.

(b) The real density dependent parameter β_R is found to be constant around unity for all the elastic scattering of composite projectiles reactions considered here indicating that the real density dependent parameter for factorized density dependent form does not depend on the incident energy nor the target nucleus. The dependence of this parameter on the projectile density is not confirmed since the two considered projectiles have similar distribution densities. The imaginary density dependent parameter β_I decreases with increasing energy and reaches zero in the case of ^{3}He+^{12}C at 119 and 217 MeV, i.e., 39.67 and 72.33 MeV/N, respectively, which may indicate a decreasing dependence of β_I as energy increases.

(c) At lower energies, although $N_R=N_I=1$, we consider that the behavior of parameters at these lower energies are not true because of (i) strong absorption effect of the imaginary part of JLM (leading to small values of N_I, for NDDP set, and sudden increasing of β_I, for DDP set, compared with energies above 16 MeV/N, e.g., $\alpha+{}^{16}$O reaction), (ii) nonconfirmed validity of JLM(R+I) at lower energies (leading to less satisfactory fitting at limited angles, e.g., ^{3}He+^{12}C and ^{3}He+^{16}O reactions discussed above).

(d) We can see that the values of β_I for ^{3}He particle reactions are slightly smaller than the corresponding values for α-particle reactions around the same energy per nucleon which may indicate that the imaginary potential is more sensitive than the real potential of JLM interaction for different projectile densities.

(4) It can be seen from Figs. 1–8 that the elastic scattering of investigated reactions exhibits the picture of nuclear rainbow scattering with a broad maximum in a specific range of energies. The energy dependence of rainbow scattering is found, since as the energy increases the rainbow maximum angle is shifted to forward angles into the narrow diffraction region. In the present work, JLM(R+I) potential describes well the rainbow scattering behavior at projectile energies $E_{\rm lab}\geqslant 20$ MeV/N, with renormalization factors (N_R and N_I) equal unity.

(5) JLM(R+I) potential reproduces quite well the reaction cross sections σ_R for investigated reactions and describes well the energy dependence of σ_R for energies greater than 16 MeV/N.

Finally, use of JLM interaction in analysis of data for other projectiles, targets, and energies is required.

ACKNOWLEDGMENT

Many thanks are due to Dr. A. L. Elattar, Department of Physics, Faculty of Science, Assiut University, Assiut, Egypt, for reading the manuscript.

[1] A. Hogenbirk, H. P. Blok, F. A. Jansen, and J. J. A. Zalmastra, Phys. Lett. B **223**, 282 (1989).
[2] A. Hogenbirk, Ph.D. thesis, Vrije Universiteit, Amsterdam, 1989; (private communication).
[3] J.-P. Jeukenne, A. Lejeune, and C. Mahaux, Phys. Rev. C **16**, 80 (1977); **15**, 10 (1977); **10**, 2392 (1974).
[4] I. Pecina, R. Anne, D. Bazin, C. Borcea, V. Borrel, F. Carstoiu, J. M. Corre, Z. Dlouhy, A. Fomitchev, D. Guillemaud-Mueller, H. Keller, A. Kordasz, M. Lewitowicz, S. Lukyanov, A. C. Mueller, Yu. Penionzhkevich, P. Roussel-Chomaz, M. G. Saint-Laurent, N. Skobelev, O. Sorlin, and O. Tarasov, Phys. Rev. C **52**, 191 (1995).
[5] H. Abele, H. J. Hauser, A. Körber, W. Leitner, R. Neu, H. Plappert, T. Rohwer, G. Staudt, M. Staßer, S. Welte, M. Walz, P. D. Eversheim, and F. Hinterberger, Z. Phys. A **326**, 373 (1987).
[6] B. I. Kuznetsov and I. P. Chernov, Sov. J. Nucl. Phys. **20**, 340 (1975).
[7] F. Michel, J. Albinski, P. Belery, Th. Delbar, Gh. Grégoir, B. Tasiaux, and G. Reidemeister, Phys. Rev. C **28**, 1904 (1983).
[8] E. H. Esmael, S. A. H. Abou Steit, M. E. M. Zedan, and M. Y. M. Hassan, J. Phys. G **17**, 1755 (1991).
[9] R. Lichtenthäler, F. A. C. C. Villari, A. Lépine-Szily, and L. C. Gomes, Phys. Rev. C **44**, 1152 (1991).
[10] A. S. Goncharov, A. S. Dem'yanova, I. Yu. Zayats, A. P. Il'in, A. V. Kuznichenko, L. V. Mikhallov, A. V. Mokhnach, A. A. Ogloblin, G. M. Onishchenko, O. A. Ponkratenko, A. G. Prokopets, A. T. Rudchik, V. K. Chernievskii, and A. A. Shvedov, Sov. J. Nucl. Phys. **54**, 552 (1991).
[11] H. Abele and G. Staudt, Phys. Rev. C **47**, 742 (1993).
[12] A. S. Dem'yanova, E. F. Svinareva, S. A. Goncharov, S. N. Ershov, F. A. Gareev, G. S. Kazacha, A. A. Ogloblin, and J. S. Vaagen, Nucl. Phys. **A542**, 208 (1992).
[13] G. R. Satchler and W. G. Love, Phys. Rep. **55**, 183 (1979).
[14] A. M. Kobos, B. A. Brown, P. E. Hodgson, G. R. Satchler, and A. Budzanowski, Nucl. Phys. **A384**, 65 (1982).
[15] A. M. Kobos, W. Haider, and J. R. Rook, Nucl. Phys. **A417**, 256 (1984).
[16] M. El-Azab Farid and G. R. Satchler, Nucl. Phys. **A438**, 525 (1985).
[17] M. E. Brandan and G. R. Satchler, Nucl. Phys. **A487**, 477 (1988).
[18] A. K. Chaudhuri, Nucl. Phys. **A449**, 243 (1986); **A459**, 417 (1986).
[19] J. Cook and R. J. Griffiths, Nucl. Phys. **A366**, 27 (1981); J. Cook, *ibid.* **A465**, 207 (1987).

[20] D. K. Srivastava, Phys. Lett. **122B**, 18 (1983); D. K. Srivastava, N. K. Ganguly, and P. E. Hodgson, *ibid.* **51B**, 439 (1974); D. K. Srivastava, D. N. Basu, and N. K. Ganguly, *ibid.* **124B**, 6 (1983).
[21] W. Haider, A. M. Kobos, and J. R. Rook, Nucl. Phys. **A480**, 1 (1988); H. Ngô, *ibid.* **A390**, 198 (1982); J. W. Negele and K. Yazaki, Phys. Rev. Lett. **47**, 71 (1981).
[22] W. D. Myers, Nucl. Phys. **A204**, 465 (1973).
[23] Shen Qing-biao, Feng Da-chun, and Zhuo Yi-zhong, Phys. Rev. C **43**, 2773 (1991).
[24] S. A. E. Khallaf, A. E. Belal, and S. E. M. Abu-kamer, Proc. Math. Phys. Soc. Egypt **51**, 27 (1981).
[25] P. D. Kunz, DWUCK4 program, University of Colorado, 1969 (unpublished).
[26] G. Hauser, R. Löhken, H. Rebel, G. Schatz, G. W. Schweimer, and J. Specht, Nucl. Phys. **A128**, 81 (1969).
[27] S. M. Smith, G. Tibell, A. A. Cowley, D. A. Goldberg, H. G. Pugh, W. Reichart, and N. S. Wall, Nucl. Phys. **A207**, 273 (1973).
[28] B. Tatischeff and I. Brissaud, Nucl. Phys. **A155**, 89 (1970).
[29] B. G. Harvey, E. J.-M. Rivet, A. Springer, J. R. Meriwether, W. B. Jones, J. H. Elliott, and P. Darriulat, Nucl. Phys. **52**, 465 (1964).
[30] Hans-Jochen Trost, Peter Lezoch, and Udo Strohbusch, Nucl. Phys. **A462**, 333 (1987).
[31] A. S. Dem'yanova, E. F. Svinareva, S. A. Goncharov, S. N. Ershov, F. A. Gareev, G. S. Kazacha, A. A. Ogloblin, and J. S. Vaagen, Nucl. Phys. **A542**, 208 (1992).
[32] Tetsumi Tanabe, Katsuji Koyama, Masaharu Yasue, Hideaki Yokomizo, Kenji Sato, Jun Kokame, Norihiko Koori, and Seiji Tanaka, J. Phys. Soc. Jpn. **41**, 361 (1976).
[33] M. Hyakutake, I. Kumabe, M. Fukada, T. Komatuzaki, T. Yamagata, M. Inolue, and H. Ogata, Nucl. Phys. **A333**, 1 (1980).
[34] N. Willis, I. Brissaud, Y. Le Bornec, B. Tatischeff, and G. Duhamel, Nucl. Phys. **A204**, 454 (1973).
[35] J. Vernotte, G. Berrier-Ronsin, J. Kalifa, and R. Tamisier, Nucl. Phys. **A390**, 285 (1982).
[36] Y.-W. Lui, O. Karban, S. Roman, R. K. Bhowmik, J. M. Nelson, and E. C. Pollacco, Nucl. Phys. **A333**, 205 (1980).
[37] L. Alvarez and G. Pálla, J. Phys. G **8**, 987 (1982).
[38] V. V. Adodin, N. T. Burtebaev, and A. D. Duisebaev, Sov. J. Nucl. Phys. **55**, 319 (1992).
[39] H.-J. Trost, A. Schworz, U. Feindt, F. H. Heimlich, S. Heinzel, J. Hintze, F. Körber, R. Lekebusch, P. Lezoch, G. Möck, W. Paul, E. Roick, M. Wolff, J. Worzeck, and U. Strahbusch, Nucl. Phys. **A337**, 377 (1980).
[40] A. Lejeune and P. E. Hodgson, Nucl. Phys. **A295**, 301 (1978).
[41] Li Qing-Run and Yang Yong-Xu, Nucl. Phys. **A561**, 181 (1993).
[42] M. N. Harakeh, A. R. Arends, M. J. A. De Voigt, A. G. Drentje, S. Y. Van Der Werf, and A. Van Der Woude, Nucl. Phys. **A265**, 189 (1976).
[43] N. Burtebaev, A. D. Duisebaev, G. N. Ivanov, and S. B. Sakuta, Phys. At. Nucl. **58**, 540 (1995).
[44] R. M. DeVries and J. C. Peng, Phys. Rev. Lett. **43**, 1373 (1979); R. M. DeVries and J. C. Peng, Phys. Rev. C **22**, 1005 (1980).